Voltage- and Time-dependent K+ Channel Currents in the Basolateral Membrane of Villus Enterocytes Isolated from Guinea Pig Small Intestine

HIROSHI TATSUTA*, SHUNJI UEDA*, SHIGERU MORISHIMA*, and YASUNOBU OKADA‡

From the *Department of Internal Medicine, and ‡Department of Physiology, Faculty of Medicine, Kyoto University, Kyoto 606-01, Japan

ABSTRACT   Patch-clamp studies were carried out in villus enterocytes isolated from the guinea pig proximal small intestine. In the whole-cell mode, outward K+ currents were found to be activated by depolarizing command pulses to -45 mV. The activation followed fourth order kinetics. The time constant of K+ current activation was voltage-dependent, decreasing from ~ 3 ms at -10 mV to 1 ms at $+50$ mV. The K+ current inactivated during maintained depolarizations by a voltage-independent, monoexponential process with a time constant of ~ 470 ms. If the interpulse interval was shorter than 30 s, cumulative inactivation was observed upon repeated stimulations. The steady state inactivation was voltage-dependent over the voltage range from -70 to -30 mV with a half inactivation voltage of -46 mV. The steady state activation was also voltage-dependent with a half-activation voltage of -22 mV. The K+ current profiles were not affected by chelation of cytosolic Ca^{2+}. The K+ current induced by a depolarizing pulse was suppressed by extracellular application of TEA^+, Ba^{2+}, 4-aminopyridine or quinine with half-maximal inhibitory concentrations of 8.9 mM, 4.6 mM, 86 μM and 26 μM, respectively. The inactivation time course was accelerated by quinine but decelerated by TEA^+, when applied to the extracellular (but not the intracellular) solution. Extracellular (but not intracellular) applications of verapamil and nifedipine also quickened the inactivation time course with 50% effective concentrations of 3 and 17 μM, respectively. Quinine, verapamil and nifedipine shifted the steady state inactivation curve towards more negative potentials. Outward single K+ channel events with a unitary conductance of ~ 8.4 pS were observed in excised inside-out patches of the basolateral membrane, when the patch was depolarized to -40 mV. The ensemble current rapidly activated and thereafter slowly inactivated with similar time constants to those of whole-cell K+ currents. It is concluded that the basolateral

membrane of guinea pig villus enterocytes has a voltage-gated, time-dependent, Ca^{2+}-insensitive, small-conductance K^+ channel. Quinine, verapamil, and nifedipine accelerate the inactivation time course by affecting the inactivation gate from the external side of the cell membrane.

INTRODUCTION

In mammalian villus enterocytes, much indirect evidence has indicated that activation of a K^+ conductance of the basolateral membrane plays an important role in controlling the Na^+-coupled absorption of sugars and amino acids (Brown, Burton, and Sepúlveda, 1983; Brown and Sepúlveda, 1985; Montero, Calonge, Bolufer, and Ilundain, 1990). Also, activation of the K^+ conductance has been shown to be associated with a regulatory volume decrease of mammalian enterocytes after swelling induced by nutrient accumulation (MacLeod and Hamilton, 1991a) or hyposmotic challenge (Hazama and Okada, 1988; MacLeod and Hamilton, 1991b; O'Brien, Walters, and Sepúlveda, 1991). Recent patch-clamp studies have provided evidence for the presence of Ca^{2+}-activated K^+ channels in rat enterocytes (Morris, Gallacher, and Lee, 1986) and a human enterocyte line (Hazama and Okada, 1988), of inwardly rectifying K^+ channels in guinea pig enterocytes (Fargon, McNaughton, and Sepúlveda, 1990; Sepúlveda, Fargon, and McNaughton, 1991) and Necturus enterocytes (Costantin, Alcalen, De Souza Otero, Dubinsky, and Schultz, 1989), and of Ca^{2+}-independent large-conductance K^+ channels in guinea pig enterocytes (Mintenig, Monaghan, and Sepúlveda, 1991). In the present study, we have identified a new type of enterocyte K^+ channel.

Parts of these studies have been published in abstract form (Tatsuta, Itoh, Ueda, and Okada, 1991).

MATERIALS AND METHODS

Cell Preparation

A 15–20-cm length of the proximal small intestine was excised from a male guinea pig (weighing 250–300 g) under anesthesia with ether. The lumen was filled with low Cl^- HEPES-buffered saline (HBS), which was composed of (in mM) 137.5 Na-gluconate, 4.2 K-gluconate, 2.9 Ca-gluconate, 0.85 $MgSO_4$, 1 $MgCl_2$, 20 mannitol and 14 HEPES-NaOH (pH 7.3), supplemented with 0.5 mM hydroxybutyrate and 0.5 mM dithiothreitol (DTT). After ligating the tissue, the sac was incubated in the same solution for 10 min at 37°C. The luminal content was then replaced with low Cl^- HBS supplemented with 1 mg/ml bovine serum albumin (BSA) and 500 U/ml dispase. The ligated sac was again incubated in low Cl^- HBS supplemented with hydroxybutyrate and DTT for 20 min at 37°C, and then gently massaged between finger tips for 5 min. The luminal content was diluted in 30 ml of low Cl^- HBS supplemented with BSA and hydroxybutyrate. The cell suspension was centrifuged for 5 min at 600 rpm. The pellet was resuspended in 15 ml of low Cl^- HBS supplemented with BSA and hydroxybutyrate, and stored on ice until used (after 10 min to 8 h).

The viability of these enterocytes was judged to be 89% by trypan blue dye extrusion 4 h after isolation.

Solutions and Chemicals

The enterocytes were perfused with a bathing solution (at ~3 ml/min) through a chamber (1 ml) by gravity feed from a reservoir. The composition of the control bathing solution was (in

mM): 4.2 KCl, 137.5 NaCl, 0.9 CaCl$_2$, 2.0 MgCl$_2$, 20 mannitol and 14 HEPES-NaOH (pH 7.4). In some experiments, KCl was substituted for NaCl on an equimolar basis. The Cl⁻-free bathing solution was composed of (in mM): 4.2 K-gluconate, 137.5 Na-gluconate, 3.4 MgSO$_4$, 2.9 Ca-gluconate, 20 mannitol and 14 HEPES-NaOH (pH 7.4).

The standard pipette solution contained (in mM) 147 KCl, 0.455 CaCl$_2$, 1 MgCl$_2$, 4 BAPTA-K$_4$ (Dojindo Laboratories, Kumamoto, Japan) and 20 HEPES-NaOH (pH 7.3, pCa 7.9). When necessary, intracellular Ca^{2+} ions were buffered to pCa 10 with 4 mM BAPTA and 4.5 μM contaminating Ca^{2+} (determined with Ca^{2+}-selective electrodes). In some experiments, the cytosol was dialyzed with a K⁺-free, Cs⁺-rich pipette solution containing (in mM) 147 CsCl, 1 MgCl$_2$, 1 EGTA and 20 HEPES-NaOH (pH 7.3, pCa 9.5).

4-Aminopyridine (4-AP) and verapamil hydrochloride were directly dissolved in the bathing or pipette solution. Quinine hydrochloride and nifedipine hydrochloride were applied to the cell after diluting the stock solutions (made up in DMSO) with the bathing or pipette solution. The vehicle alone had no effect on membrane currents at the concentrations employed (<0.1%). When TEA⁺ and Ba^{2+} were applied to the cell, NaCl in the bathing or pipette solution was replaced with TEA-Cl and BaCl$_2$ at ratios of 1:1 and 2:3, respectively.

Unless otherwise stated, the chemicals employed were purchased from Nacalai Tesque (Kyoto, Japan).

Current Recordings

Currents were recorded with tight-seal patch electrodes using a patch-clamp amplifier (LIST, EPC-7) at room temperature (22–25°C). Single channel recordings were made in the inside-out patches from the brush border-free membrane of enterocytes. Whole-cell current recordings were carried out, as described previously (Kubo and Okada, 1992). The resistance of a patch electrode filled with a standard pipette solution was 3–5 MΩ. Capacitance (10–25 pF) and series resistance were compensated electronically. Unless otherwise stated, the standard pipette solution and the control bathing solution were employed as the intracellular solution (in the bath for inside-out patch recordings, in the pipette for whole-cell recordings) and as the extracellular solution (in the pipette for inside-out patch recordings, in the bath for whole-cell recordings), respectively. The resting membrane potential of enterocytes determined in the whole-cell current clamp mode was −47.3 ± 1.2 mV (n = 79) in the control bathing solution.

The currents were filtered at 3 kHz and recorded using a pulse-code modulator (Sony PCM-501ES). Off-line data analysis was made at a sampling frequency of 0.167–20 kHz using a personal computer (NEC PC9801FS) via a 12-bit A/D converter (Canopus, ADX-98E).

Voltage pulses were generated by an electronic stimulator (SEN-3201, Nihon Kohden, Tokyo, Japan) and a computer-aided pulse generator (Shoshin EM, Type OI-8, Okazaki, Japan). To record voltage-dependent current activation, a series of command pulses (5-, 10- or 20-mV steps of 30-, 1,500- or 4,000-ms duration) were applied from the holding potential at −90, −75, −70, or −50 mV to a variety of voltage levels (−150 to +65 mV). The interval between pulses was usually set at 56–60 s to eliminate cumulative inactivation of the currents. To record the voltage-dependence of tail currents, deactivation of outward currents which had been induced by 100-ms voltage steps to +50 mV was initiated by step back to various potentials for 1 s at 1-min intervals. The voltage-dependence of steady state activation was measured by varying the depolarizing voltage commands (−70 to +50 mV). The steady state inactivation properties were determined by measuring the current in response to a fixed voltage command of +10 mV after various holding potentials (−110 to −10 mV). The leak current component was not compensated.

Curve-fittings were performed by nonlinear least squares using commercial software (Sigma Plot, Jandel Scientific, Corte Madera, CA) or *ad hoc* programs. Data are given as means ± SEM with the number of observations (n) in parenthesis. Statistical significance of difference between means was evaluated by t test. The level of significance was set at P < 0.05.

RESULTS

Cell Morphology

The isolated cell has a columnar to oval appearance, having a well-defined brush border at one pole immediately after isolation. Most cells gradually became spherical within 60 min at room temperature, the brush border eventually becoming invisible in spherical cells (Fig. 1 A) . The cell diameter ranged from 15 to 20 μm. Fig. 1 B shows the histological appearance of the intestinal segment after enzymatic treatment. The villus region had intact villus cores but no remaining epithelial cells, whereas the crypt region was covered with intact monolayer epithelial cells. These
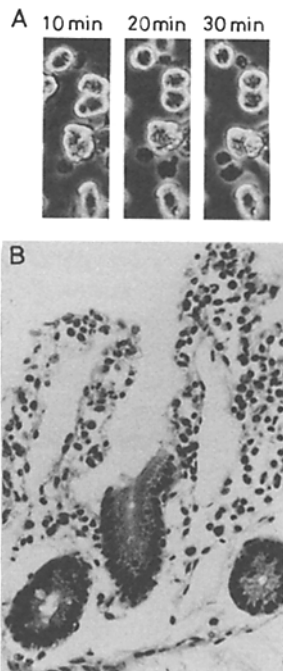

FIGURE 1. Micrographs of isolated enterocytes and the remaining tissue of guinea pig small intestine. (A) Phase contrast micrographs of isolated enterocytes after incubation in the control bathing solution at room temperature for 10, 20, and 30 min. Brush border structures are visible at one pole of the cells (arrowheads). (B) A hematoxylin-eosin stained section of the small intestine after enzymatic treatment for enterocyte isolation. Representative of histological specimens from nine animals.

results demonstrate that the isolated cells are derived exclusively from villus enterocytes.

Voltage-dependent Whole-Cell K⁺ Currents

Using the whole-cell recording technique, inactivating outward currents were consistently observed in both enterocytes with and without visible brush borders upon application of depolarizing command potentials above −50 mV from a holding potential of −70 or −90 mV. As shown in Fig. 2, the depolarization-induced outward current was rapidly activated and thereafter slowly inactivated. There was no indication of any inward currents upon either depolarization or hyperpolarization.

Activation of the current proceeded with a characteristic delay and sigmoidal time course (Fig. 2 Aa). The activation phase of the currents was best fitted by the
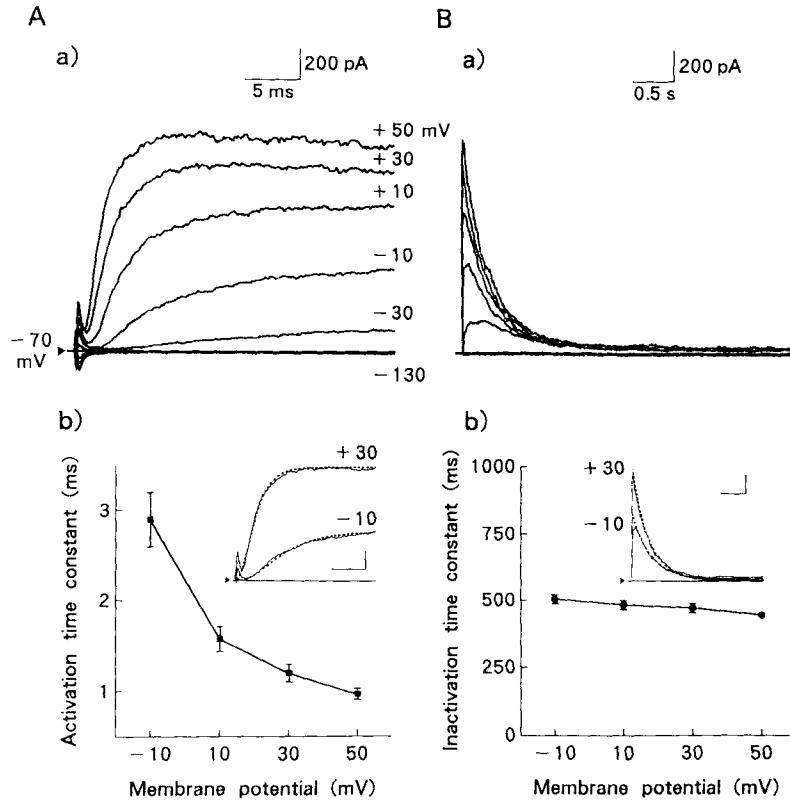
FIGURE 2. Voltage-gated whole-cell currents recorded from guinea pig villus enterocytes. Bath, control bathing solution. Pipette, standard pipette solution. The arrowhead and horizontal lines represent the zero current level. (*A*) Activation kinetics. (*a*) Representative currents in response to 30-ms pulses applied from a holding potential of -70 mV to potentials ranging from -130 to $+50$ mV in 20-mV increments. The parameters fitted to Eq. 1 were as follows: I_{max} = 1,540, 1,358, 1,001 and 520 pA; m = 4.3, 3.5, 3.7, and 3.9; τ_a = 1.2, 1.8, 2.5, and 4.3 ms; at $+50$, $+30$, $+10$, and -10 mV, respectively. (*b*) The mean activation time constant plotted as a function of voltage (n = 8). (*Inset*) The examples of fitting (*broken lines*) for currents recorded at -10 and $+30$ mV. Scales represent 5 ms and 200 pA. (*B*) Inactivation kinetics. (*a*) Representative currents in response to 4-s pulses applied from a holding potential of -70 mV to potentials ranging from -130 to $+50$ mV in 20-mV increments. The inactivation time courses could be fitted by a single exponential function with time constants (τ_i) of 390, 396, 408, and 421 ms at $+50$, $+30$, $+10$, and -10 mV, respectively. (*b*) The mean τ_i values plotted vs voltage (n = 35). (*Inset*) The examples of fitting (*broken lines*) for currents recorded at -10 and $+30$ mV. Scales represent 0.5 s and 200 pA.

equation:

$$I = I_{max}[1 - \exp(-t/\tau_a)]^m \tag{1}$$

with the m value of around four (Fig. 2 *Ab*, *inset*). As shown in Fig. 2 *A(b)*, the activation time constant (τ_a) was dependent on voltage. The current activated more promptly, when the membrane potential became more positive.

The inactivation phase of the outward currents could be adequately fitted by a single exponential (Fig. 2 *Bb*, *inset*). As shown in Fig. 2 *B(b)*, the inactivation time constant (τ_i) was little dependent on voltage in the range between −10 and +50 mV at which the conductance is completely activated (see Fig. 5). The recovery from inactivation was time dependent. If the interpulse interval was shorter than 30 s, cumulative inactivation was observed upon repetitive stimulations (data not shown).

The peak current-voltage relationship is illustrated in Fig. 3 *A* (*open circles*). When the control bathing solution was replaced with a Cl⁻-free solution, the current profile did not change, as shown in Fig. 3 *A* (*inset and filled circles*). When K⁺ was substituted for Cs⁺ in the pipette solution, the outward current was completely abolished ($n = 4$, data not shown). When the extracellular K⁺ concentration ([K⁺]ₒ) was increased to
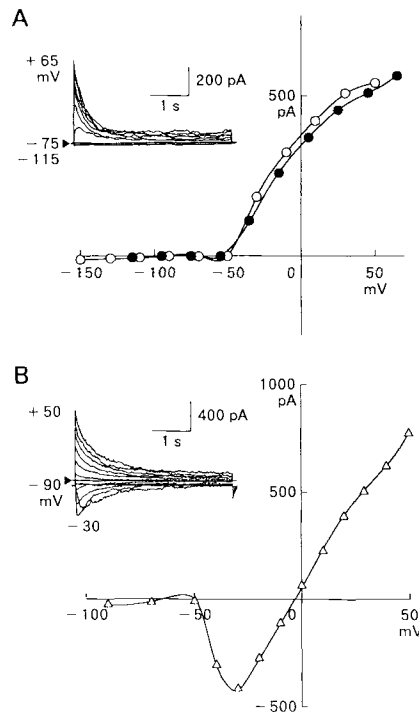

FIGURE 3. Representative peak current-voltage relationship. Arrowheads and horizontal lines represent the zero current level. Pipette, standard pipette solution. (*A*) Recorded with 4.2 mM K⁺ in the control bathing solution (*open circles:* holding potential −90 mV) and in Cl⁻-free bathing solution (*filled circles:* holding potential −75 mV) in a single villus enterocytes. (*Inset*) The current traces in the absence of Cl⁻ in the bathing solution. The command potential range and the holding potential are indicated. (*B*) Recorded with 141.7 mM K⁺ (holding potential −90 mV) in another villus enterocyte. (*Inset*) The current traces.

141.7 mM, inward currents were activated in response to negative voltage steps of less than −50 mV (Fig. 3 *B*). The reversal potential was −4.2 ± 0.5 mV ($n = 4$), close to E_K (−3.6 mV), indicating that the principal carrier of the current was K⁺. This inference was confirmed by analysis of the tail currents. In 4.2 mM [K⁺]ₒ, the tail currents reversed at −84.0 ± 2.2 mV ($n = 5$) (Fig. 4 *A*). When [K⁺]ₒ was increased by 10-fold, the reversal potential shifted to −26.5 ± 1.4 mV ($n = 5$), in the manner expected of a K⁺-selective channel (Fig. 4 *B*).

The K⁺ current profiles were not affected by the intracellular application of ATP (1 mM, $n = 3$) or by chelation of cytosolic Ca²⁺ (pCa 10, $n = 8$).

Fig. 5 *A* (*circles*) shows the normalized peak K⁺ conductance as a function of voltage. The conductance increased steeply with depolarization and saturated at

positive potentials. The continuous line through the data points represents the best fit to a Boltzmann distribution:

$$G/G_{max} = 1/[1 + \exp\{(V - V_{1/2})/k\}] \tag{2}$$

The half-activation voltage ($V_{1/2}$) was -21.7 ± 0.8 mV ($n = 24$). The steepness of the voltage-dependence (k) was -9.3 ± 0.4, suggesting that the effective gating charge ($-RT/Fk$) is more than 2.7. Because the limiting slope of the semilogarithmic steady state activation curve is a better measure of the effective gating charge (Almers,
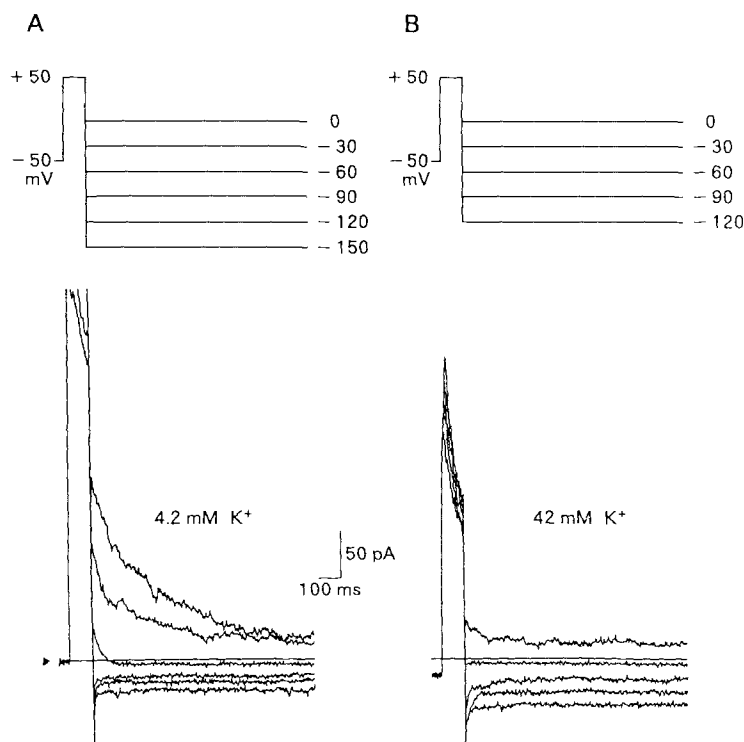

FIGURE 4.   Tail current analysis at 4.2 mM K^+ (A) and 42 mM K^+ (B). Deactivating tail currents (*lower*) recorded by the double-pulse protocol (*upper*). Capacitative components (time constant of ~ 4 ms) could be evaluated by fitting the curves with double exponential functions. Arrowheads and horizontal lines represent the zero current level.

1978), such a plot was constructed from currents in response to command pulses more positive than -45 mV in 5-mV steps. As shown in Fig. 5 B, at potentials more negative than -30 mV the conductance grew e-fold in 4.1 mV, indicating that the effective gating charge is at least 6.2 equivalents.

The voltage dependence of steady state inactivation was studied by varying the holding potential prior to recording the K^+ current at a constant test potential ($+10$ mV). As shown in Fig. 5 A (*squares*), the data points could again be fitted with a Boltzmann function (h_∞ = Eq. 2). The half-inactivation voltage ($V_{1/2}$) was -45.6 ± 0.5

mV (n = 21). The slope factor (k) was 3.9 ± 0.2, suggesting the effective gating charge is more than 6.5.

Sensitivity to K^+ Channel Blockers

The outward K^+ channel currents were found to be sensitive to a variety of K^+ channel blockers. Extracellular applications of TEA^+, Ba^{2+} and quinine suppressed both the peak and sustained K^+ currents (Fig. 6 A) without exhibiting use-dependent effects (Fig. 6 Ba). The time needed for attaining steady state inhibition was 3–5 min for Ba^{2+} and 2–4 min for TEA^+ and quinine. Extracellular 4-AP exhibited use-
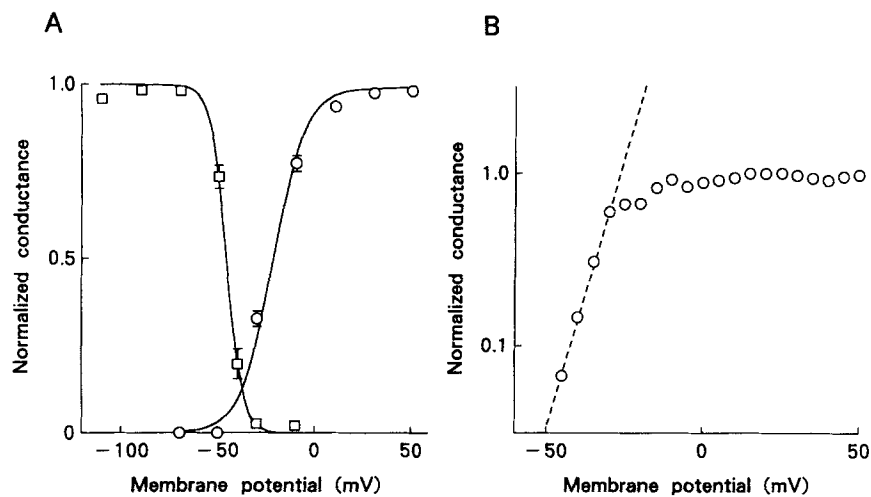

FIGURE 5. Voltage dependency of the activation and inactivation of whole-cell K^+ currents in guinea pig villus enterocytes. The steady state activation properties were determined by observing the current with a depolarizing command (−70 to +50 mV) after a fixed holding potential at −90 mV. Steady state inactivation was observed by holding the cell for more than 1 min at −110 to −10 mV, and applying a single test pulse to +10 mV. (A) Steady state activation and inactivation curves. Symbols (with bars) represent mean normalized conductances (±SEM) of 21–24 enterocytes. The Boltzmann function (Eq. 2) was fitted to the data. $V_{1/2}$ and k of the activation curve (circles) were −21.6 mV and −8.3, respectively. For the inactivation curve (squares), $V_{1/2}$ = −45.7 mV and k = 4.3. (B) A semilogarithmic steady state activation curve recorded in a single enterocyte by applying 4-s step pulses in 5-mV increments. The limiting slope is shown by a broken line.

dependent inhibition. Even 5 min after exposure to 4-AP, no change in the K^+ current was observed upon the first application of a command pulse, whereas distinct suppression was found upon subsequent applications of command pulses (Fig. 6 Bb). The inhibitory effects of these K^+ channel blockers were reversible after wash-out. The extracellular concentrations required for 50% inhibition (IC_{50}) of the peak K^+ current were 8.9 mM, 4.6 mM, 86 μM and 26 μM for TEA^+, Ba^{2+}, 4-AP and quinine, respectively (Fig. 6 C). Intracellular applications of TEA^+ (10 mM), Ba^{2+} (5 mM) and 4-AP (1 mM) abolished the K^+ current, whereas intracellular quinine (100 μM) failed to block the K^+ current (n = 3–5, data not shown). The outward K^+ currents were not affected by extracellular applications of Cs^+ (100 mM) or glibenclamide (10 μM).

A

a) TEA^+ b) Ba^{2+} c) 4-AP   d) Quinine

|400 pA

+50 mV   1 s

control   control   control   control

-70▸
-130

10 mM   5 mM   0.1 mM   20 μ M

100 mM   50 mM   1 mM   100 μ M

B   C

a) 20 mM TEA^+

+10 |200 pA

1 s

-70▸ mV

b) 0.1 mM 4-AP

+10 |200 pA

1 s

-70▸ mV

Normalized conductance

1.0

4-AP   TEA⁺

0.5

Quinine Ba^{2+}

0

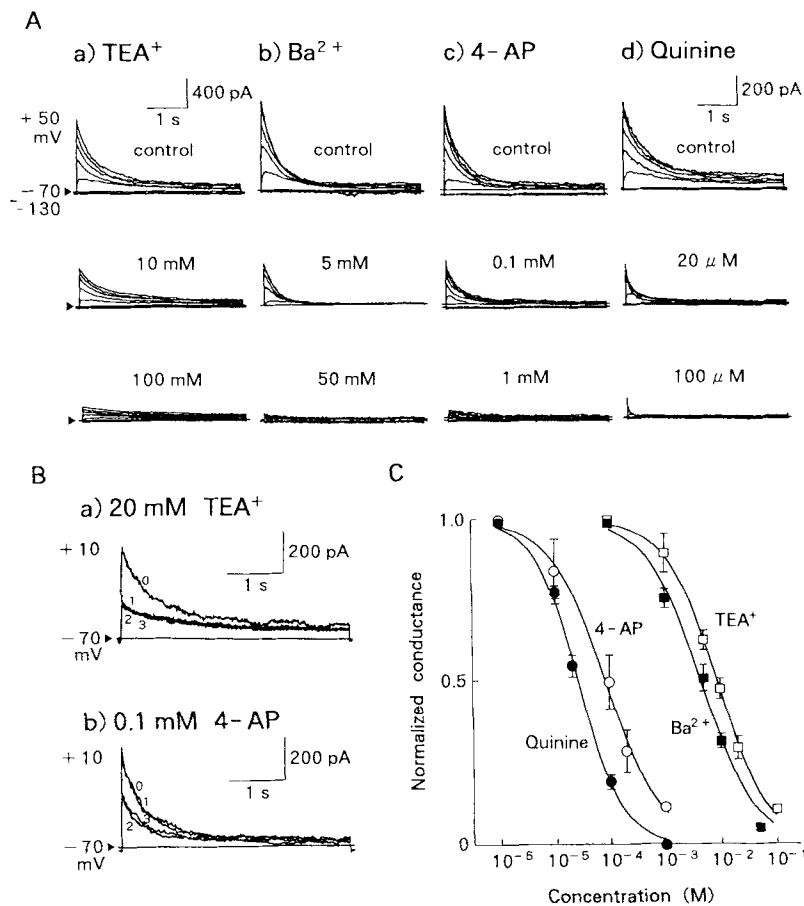10^{-6} 10^{-5} 10^{-4} 10^{-3} 10^{-2} 10^{-1}

Concentration (M)

FIGURE 6. Effects of K^+ channel blockers on whole-cell K^+ currents of guinea pig enterocytes. Arrowhead and horizontal lines represent the zero current level. (*A*) Representative traces of currents in response to 4-s pulses applied from a holding potential of −70 mV to varying potentials (−130 to +50 mV) before (*top group of traces*) and after addition of blocker to the extracellular solution (*middle and bottom groups of traces*). Blockers were TEA^+ (*a*), Ba^{2+} (*b*), 4-AP (*c*) and quinine (*d*), and concentrations were as indicated. The three traces were recorded from the same cell. (*B*) Use-dependent effects of 20 mM TEA^+ (*a*) and 0.1 mM 4-AP (*b*). Currents were elicited by 4-s pulses from a holding potential of −70 mV to +10 mV before (*0*), 5 min (*1*), 6 min (*2*) and 7 min (*3*) after drug applications. (*C*) Dose-inhibition curves. After attaining steady state inhibition, the peak currents were recorded at 10 mV and normalized to the peak current before drug applications. The data points (with bars) represent mean values (with SEM) of three to eight experiments. (*Curves*) Fits of the equation $y = 1 - x^n/(IC_{50}^n + x^n)$ to the data. The Hill coefficients (*n*) were 1.09, 0.86, 0.91, and 0.96 for quinine, 4-AP, Ba^{2+} and TEA^+, respectively.

After attaining steady-state inhibition of the peak K^+ current amplitude, effects of extracellular K^+ channel blockers on activation and inactivation kinetics were examined at concentrations near IC_{50}. The K^+ channel blockers had no significant effects on the time course of activation. The activation time constants at −10 mV

were 2.0 ± 0.2 ms ($n = 4$), 2.3 ± 0.2 ms ($n = 4$), 1.7 ± 0.4 ms ($n = 3$) and 1.8 ± 0.2 ms ($n = 4$) in the presence of 10 mM TEA^+, 5 mM Ba^{2+}, 100 μM 4-AP and 20 μM quinine, respectively. These values were not significantly different from the control value in the absence of blockers (2.0 ± 1.2 ms, $n = 15$). Quinine and TEA^+ had opposite effects on the time course of inactivation. TEA^+ (10 mM) slowed down inactivation, whereas quinine (20 μM) accelerated it (Fig. 7). In contrast, neither Ba^{2+} (5 mM) nor 4-AP (100 μM) affected the inactivation time course (Fig. 7). Neither activation nor inactivation kinetics were affected by intracellular application of TEA^+ (1 mM), Ba^{2+} (1 mM), 4-AP (0.1 mM) or quinine (0.1 mM).

In the presence of extracellular TEA^+ (10 mM), Ba^{2+} (5 mM) or 4-AP (100 μM) there was no significant change in the steady state parameters of current activation and inactivation ($n = 3$–4, data not shown). In the presence of quinine (20 μM), however, the steady state inactivation curve was shifted to the left or more negative holding potentials, significantly altering the $V_{1/2}$ value from -44.8 ± 0.7 to -50.4 ± 0.8 mV ($n = 4$).
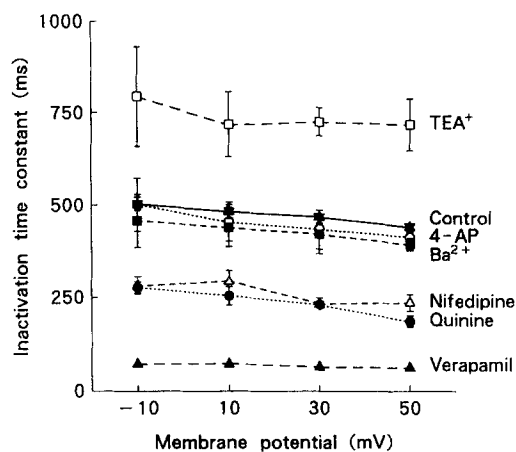

FIGURE 7. Effects of K^+ channel blockers and Ca^{2+} channel blockers on the inactivation time constants of whole-cell K^+ currents of guinea pig enterocytes. Data points and bars represent means and SEM, respectively. Control (*asterisks*; $n = 37$). TEA^+ (*open squares*; 10 mM, $n = 6$). 4-AP (*open circles*; 0.1 mM, $n = 5$). Ba^{2+} (*filled squares*; 5 mM, $n = 7$). Quinine (*filled circles*; 20 μM, $n = 8$). Nifedipine (*open triangles*; 20 μM, $n = 4$). Verapamil (*filled triangles*; 20 μM, $n = 5$).

Sensitivity to Ca^{2+} Channel Blockers

Inactivation of the K^+ current was also sensitive to the Ca^{2+} channel blockers, verapamil and nifedipine. Extracellular application of either blocker resulted in acceleration of inactivation (Figs. 7 and 8 A) in a concentration-dependent manner (Fig. 8 B) without use-dependent effects (data not shown). At +10 mV, verapamil markedly reduced the inactivation time constant (by $52 \pm 5\%$ ($n = 5$) at 5 μM and $87 \pm 2\%$ ($n = 5$) at 20 μM), but had little effect on the peak amplitude (by $-9 \pm 4\%$ ($n = 5$) at 5 μM and $-11 \pm 5\%$ ($n = 5$) at 20 μM). Similarly, nifedipine significantly reduced the time constant of inactivation, but had no effect on the peak amplitude. Nifedipine reduced the time constant of inactivation at +10 mV to $65 \pm 5\%$ ($n = 4$) of the control value at 10 μM and to $53 \pm 4\%$ ($n = 4$) at 20 μM. In contrast, the peak amplitude was inhibited by nifedipine at 10 and 20 μM by only $2 \pm 2\%$ ($n = 4$) and $19 \pm 8\%$ ($n = 4$), respectively. The effects of these drugs on the inactivation kinetics were partially reversible after wash-out. Neither verapamil nor nifedipine affected the time constant of K^+ current activation.
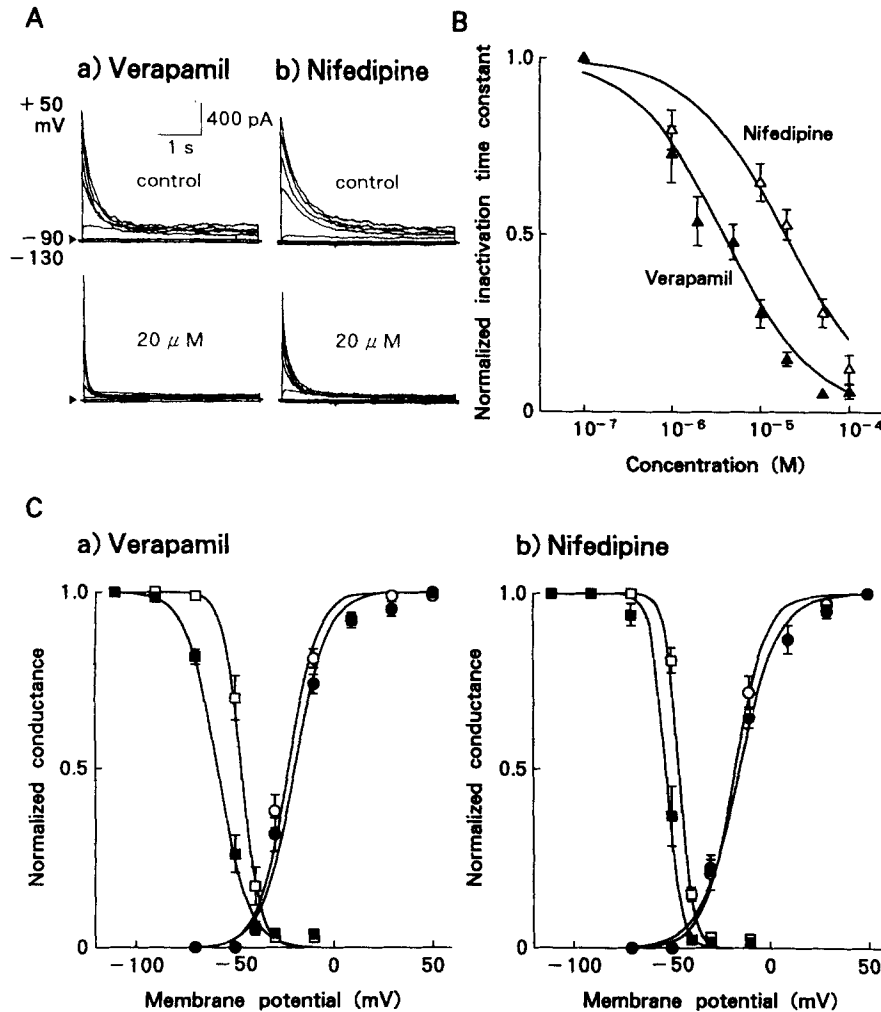
FIGURE 8. Effects of Ca²⁺ channel blockers on whole-cell K⁺ currents in guinea pig entero-cytes. (*A*) Representative traces of currents in response to 4-s pulses applied from a holding potential of −90 mV to various potentials (−130 to +50 mV) before (*upper traces*) and after (*lower traces*) drug addition to the extracellular solution. Verapamil (*a*) and nifedipine (*b*) were added at the indicated concentrations. The two traces were recorded from the same cells. Arrowheads and horizontal lines represent the zero current level. (*B*) Dose-response curves for the effects of verapamil (*filled triangles*) and nifedipine (*open triangles*) on the inactivation time constants. After obtaining steady-state effects with the drugs, the inactivation time constants were calculated and normalized to those before drug addition. Means ± SEM (*n* = 3–10). The Hill coefficients (*n*) were 0.87 for verapamil and 0.83 for nifedipine. The 50% effective concentrations were 3.1 μM for verapamil and 17 μM for nifedipine. (*C*) Steady state activation curves (*circles*) and inactivation curves (*squares*) in the absence (*open symbols*) and presence (*filled symbols*) of 20 μM verapamil (*a*) or 20 μM nifedipine (*b*).

The steady state inactivation curve was significantly shifted to the left by 10.8 ± 2.1 and 9.9 ± 2.1 mV ($n = 4$) in the presence of 20 μM verapamil and 20 μM nifedipine, respectively (Fig. 8 C, squares). Verapamil (but not nifedipine) significantly altered the slope factor (k) from 4.1 ± 0.8 to 7.4 ± 0.6 ($n = 4$). However, the steady state activation parameters were not significantly affected by either of the Ca^{2+} channel blockers (Fig. 8 C, circles).
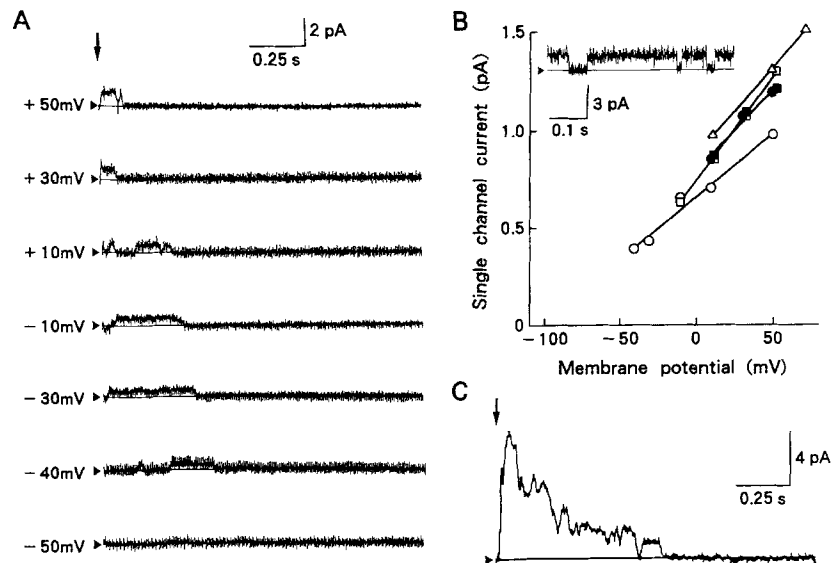

FIGURE 9. Voltage-gated single-channel currents recorded in inside-out patches excised from the brush border-free membrane of guinea pig enterocytes. Bath, standard pipette solution. Pipette, control bathing solution. Arrowheads and horizontal lines represent the zero current level. (A) Representative currents at seven different voltages (given to the left of each trace) from a single patch. Holding potential was −90 mV. Voltage steps were applied at the time indicated by the arrow. Leak and capacitative currents were subtracted from the records. (B) Single-channel current-voltage relation. Patch membranes were excised from the brush border-free membrane of three spherical enterocytes (open symbols) and two columnar enterocytes which had been isolated 10–20 min before and had clearly identifiable brush borders (filled symbols). (Inset) A current trace (corresponding to triangle at +50 mV) displayed on a faster time base. (C) The ensemble average of 14 consecutive current records in response to voltage steps to +10 mV from a holding potential of −90 mV. The data were fitted with an activation time constant of 3.5 ms and an inactivation time constant of 373 ms.

When added to the intracellular solution, both verapamil (100 μM) and nifedipine (100 μM) failed to affect the K^+ current profiles ($n = 5$ and 4, data not shown).

Single K^+ Channel Events in the Basolateral Membrane

Single-channel events were first recorded in inside-out patches of the plasma membrane of spherical enterocytes which did not have well-defined brush border structures. The most prevalent type of unitary events was an outward current that was gated by membrane depolarization to −40 mV. As shown in Fig. 9 A, larger

depolarizations induced stepwise outward events with greater current amplitude. Fig. 9 B shows a plot of current amplitude as a function of membrane potential. The current-voltage relationship was linear with a mean slope conductance of 8.4 ± 0.2 pS (n = 20). The extrapolated reversal potential (−92.0 ± 1.9 mV, n = 20) is very close to the equilibrium potential for K+ (E_K − 93 mV) and is therefore consistent with a highly selective K+ channel. Generally, the channels opened only for the first tens to hundreds of milliseconds after the depolarizing pulse. Rapid open and closed events could be observed before inactivation (Fig. 9 B, inset). After the channels inactivated, they rarely reopened during maintained depolarizations. When the patch was returned to the holding potential (−90 mV), recovery from this inactivated state required many seconds. The ensemble average of 14 such records exhibited rapid activation (with τ_a of several ms) and slow inactivation (with τ_i of ~400 ms), as shown in Fig. 9 C.

To record single-channel events in membrane patches excised from the basolateral membrane, giga seals were formed at the pole opposite to the brush border on villus enterocytes which had been stored on ice for only 10–20 min after isolation in order to minimize the possibility of redistribution of membrane proteins. Essentially identical unitary events were observed in these basolateral membrane patches (Fig. 9 B, filled symbols).

DISCUSSION

Depolarization-activated K+ channels have been described in almost all excitable cells (Hille, 1992). In the present study, using the whole-cell recording technique, similar voltage-gated K+ currents were consistently observed in villus enterocytes isolated from the guinea pig small intestine. We deduced that small-conductance K+ channels (unitary conductance 8.4 pS) found in inside-out patches of the brush border-free membrane correspond to the K+ current, based on similarities in the threshold potential, activation and inactivation kinetics and cumulative inactivation.

Activation of the K+ current could be fitted by a Hodgkin-Huxley type parameter raised to fourth power. The limiting slope of the activation curve plotted on a logarithmic ordinate predicts an effective gating charge of more than six per channel. Similar values have been estimated for the gating charges of K+ channels in a variety of excitable cells (Hodgkin and Huxley, 1952; Stanfield, 1975; Almers and Armstrong, 1980; Bezanilla and White, 1982).

Inactivation was a prominent characteristic of the enterocyte K+ channel. The inactivation phase could be fitted by a single exponential function. The inactivation process occurred over a period of hundreds of milliseconds in an almost voltage-independent manner. Recovery from inactivation was slow and took more than 30 s. Cumulative inactivation (Aldrich, Getting, and Thompson, 1979) was observed when subsequent pulses were applied before attaining complete recovery from inactivation.

These properties of the enterocyte K+ current closely resemble the n-type channel in lymphocytes; which is also activated by depolarization above −40 mV with following fourth order activation kinetics, shows slow inactivation, demonstrates cumulative inactivation and has a small single-channel conductance (DeCoursey, Chandy, Gupta, and Cahalan, 1987; Lewis and Cahalan, 1988).

The inactivation kinetics of enterocyte K+ currents was modified by a number of channel blockers. When applied to the extracellular (but not intracellular) solution, a

K^+ channel blocker (quinine) and Ca^{2+} channel blockers (verapamil and nifedipine) accelerated inactivation. Similar accelerating effects of Ca^{2+} channel blockers were found in K^+ current inactivation in human tracheal cells (Galietta, Rasola, Barone, Gruenert, and Romeo, 1991) and smooth muscle cells of rabbit small intestine (Terada, Kitamura, and Kuriyama, 1987). In contrast, extracellular TEA^+ was found to retard the K^+ channel inactivation. Decelerating effects of extracellular TEA^+ have also been found in n-type K^+ channels in lymphocytes (Grissmer and Cahalan, 1989) and in a *Shaker* K^+ channel mutant which exhibits slow inactivation kinetics due to deletion of the amino-terminal region (Choi, Aldrich, and Yellen, 1991).

Acceleration of inactivation by quinine, verapamil and nifedipine may reflect a block of K^+ channels in an open conformation. However, they did not exhibit use-dependency. In addition, the inactivation time course in the presence of either drug was adequately fitted by a single exponential, being inconsistent with the involvement of an additional "inactivating" process due to open-channel block. Furthermore, verapamil and nifedipine did not significantly alter the peak amplitude of K^+ currents. Instead, they presumably interact with the inactivation gate.

Inactivation of *Shaker* K^+ channels can be well explained by the intracellular ball-and-chain model (Armstrong and Bezanilla, 1977), in which the amino-terminal domain acts as a tethered inactivation particle that can block the internal mouth (Zagotta, Hoshi, and Aldrich, 1989). In contrast with the case of *Shaker* K^+ channel (Zagotta et al., 1989; Hoshi, Zagotta, and Aldrich, 1990), a protease (Pronase E, 2 mg/ml) applied to the intracellular (pipette) solution failed to remove the inactivation of the K^+ current (Tatsuta and Okada, unpublished observations). Because verapamil and nifedipine were effective only when applied on the extracellular side, blocker binding to an extracellular domain may cause allosteric effects on the inactivation gate at a cytosolic domain of the K^+ channel. Alternatively, the inactivation gate may reside near the external mouth of the channel. However, an extracellular ball-and-chain inactivation mechanism would seem to be unlikely, because addition of a protease to the extracellular solution did not affect inactivation of the K^+ current (Tatsuta, Tsuji, and Okada, unpublished observations). Recent results have suggested that a conformational change near the external mouth of *Shaker* K^+ channels is responsible for its slow inactivation mechanism (Choi et al., 1991).

Quinine, verapamil and nifedipine significantly shifted the steady state inactivation curve (h_∞-curve) and also shortened the inactivation time constant (τ_i). According to Hodgkin and Huxley (1952) h_∞ and τ_i are given by

$$h_\infty = \alpha_h/(\alpha_h + \beta_h) \tag{3}$$

$$\tau_i = 1/(\alpha_h + \beta_h) \tag{4}$$

where α_h and β_h are the backward and forward rate constants, respectively, for transitions between activated and inactivated states of the channel. Therefore, it appears that binding of these drugs induced alteration of the rate constant(s) presumably due to conformational changes in the channel.

So far three types of K^+ channel have been found in enterocytes of mammalian small intestine: Ca^{2+}-activated maxi-K^+ channels (unitary conductance around 250 pS) in rat (Morris et al., 1986), Ca^{2+}- and Ba^{2+}-insensitive large-conductance

(130-pS) K^+ channels in guinea pig (Mintenig et al., 1991), and inwardly rectifying TEA^+-insensitive K^+ channels in guinea pig (Sepúlveda et al., 1991). Because of its small unitary conductance (8.4 pS), Ca^{2+}-independency and sensitivity to Ba^{2+} and TEA^+, the K^+ channel identified in the present study is different from those listed above. This K^+ channel is also distinct from several K^+ channels identified by single-channel recording techniques in *Necturus* enterocytes as follows: Ca^{2+}-activated large-conductance (170-pS) K^+ channels (Sheppard, Giráldez, and Sepúlveda, 1988a), Ca^{2+}-activated intermediate-conductance (30-pS) K^+ channels (Sheppard et al., 1988b), and inwardly rectifying large-conductance (190-pS) K^+ channels (Costantin et al., 1989).

Under the present experimental conditions, the predominant whole-cell currents in villus enterocytes of the guinea pig were inactivating outward K^+ currents activated upon depolarization. Preliminary studies showed that elevation of the intracellular Ca^{2+} level induced activation of additional currents (K^+ currents flowing in both inward and outward directions, Cl^- currents, and nonselective cation currents: Tatsuta, Tsuji, and Okada, unpublished observations). However, inwardly rectifying K^+ currents have not been observed, contrary to previous observations (Costantin et al., 1989; Sepúlveda et al., 1991). The reason for this discrepancy is not clear but may be due to differences of animal species (Costantin et al., 1989) and of some other experimental conditions (Sepúlveda et al., 1991).

The whole-cell K^+ current was consistently observed in guinea pig enterocytes either before or after loosing the brush border. The corresponding single-channel activity could be recorded from membrane patches excised from the brush border-free membrane of both enterocytes with and without the brush-border at one pole. Redistribution of the membrane integral proteins after isolation of mouse enterocytes is known to take place rapidly at 37°C but is slowed by cooling at 0°C (Ziomek, Schulman, and Edidin, 1980). Essentially identical single-channel activities were recorded from the brush border-free membrane in guinea pig enterocytes which had been stored on ice for only 10–20 min after isolation. Taking these results together, it appears that the K^+ channel resides at the basolateral membrane.

The exact function of the K^+ channel has not been determined in the present study. There is an overlap of steady state activation and inactivation curves (Figs. 5 *A* and 8 *C*). The "window current" should contribute to the basal currents of villus enterocytes in the range of voltages between -50 and -30 mV. Because the resting potential of ~ -47 mV is just below the threshold potential (~ -45 mV) and close to the half-inactivation voltage (~ -46 mV), half the total population of K^+ channels would be available for activation by a small depolarizing shift of the membrane potential in guinea pig enterocytes. Transient depolarizations have been observed upon Na^+-dependent absorption of sugars and amino acids (Rose and Schultz, 1971; White and Armstrong, 1971; Okada, Tsuchiya, Irimajiri, and Inouye, 1977; Boyd and Ward, 1982; Gunter-Smith, Grasset, and Schultz, 1982; Albus, Bakker, and van Heukelom, 1983; Grasset, Gunter-Smith, and Schultz, 1983; Giráldez and Sepúlveda, 1987) and upon osmotic cell swelling in intestinal epithelial cells (Hazama and Okada, 1988). Therefore, both peak and sustained (7–8% of peak) components of the K^+ channel currents may be involved in the resetting of the resting potential (membrane repolarization) upon Na^+-coupled solute absorption and osmotic cell

swelling, K^+ recycling coupled to Na^+-K^+ pump at the basolateral membrane during active Na^+ absorption, and K^+ efflux associated with a regulatory volume decrease. In this regard, it is noteworthy that sugar absorption is known to be inhibited by verapamil in isolated enterocytes (Montero et al., 1990) and in intact ileum (Ilundain, Alcalde, Barcina, and Larralde, 1985), and by K^+ channel blockers, such as Ba^{2+} and quinine, in isolated enterocytes (Brown and Sepúlveda, 1985; Montero et al., 1990).

REFERENCE

Albus, H., R. Bakker, and J. Siegenbeek van Heukelom. 1983. Circuit analysis of membrane potential changes due to electrogenic sodium-dependent sugar transport in goldfish intestinal epithelium. *Pflügers Archiv.* 398:1–9.

Aldrich, R. W., Jr., P. A. Getting, and S. H. Thompson. 1979. Inactivation of delayed outward current in molluscan neurone somata. *Journal of Physiology.* 291:507–530.

Almers, W. 1978. Gating currents and charge movements in excitable membranes. *Reviews of Physiology, Biochemistry, and Pharmacology.* 82:96–190.

Almers, W., and C. M. Armstrong. 1980. Survival of K^+ permeability and gating currents in squid axons perfused with K^+-free media. *Journal of General Physiology.* 75:61–78.

Armstrong, C. M., and F. Bezanilla. 1977. Inactivation of the sodium channel. II. Gating current experiments. *Journal of General Physiology.* 70:567–590.

Bezanilla, F., and M. M. White. 1982. Gating currents associated with potassium channel activation. *Nature.* 296:657–659.

Boyd, C. A. R., and M. R. Ward. 1982. A micro-electrode study of oligopeptide absorption by the small intestinal epithelium of *Necturus maculosus. Journal of Physiology.* 324:411–428.

Brown, P. D., K. A. Burton, and F. V. Sepúlveda. 1983. Transport of sugars or amino acids increases potassium efflux from isolated enterocytes. *FEBS Letters.* 163:203–206.

Brown, P. D., and F. V. Sepúlveda. 1985. Potassium movements associated with amino acid and sugar transport in enterocytes isolated from rabbit jejunum. *Journal of Physiology.* 363:271–285.

Choi, K. L., R. W. Aldrich, and G. Yellen. 1991. Tetraethylammonium blockade distinguishes two inactivation mechanisms in voltage-activated K^+ channels. *Proceedings of the National Academy of Sciences, USA.* 88:5092–5095.

Costantin, J., S. Alcalen, A. De Souza Otero, W. P. Dubinsky, and S. G. Schultz. 1989. Reconstitution of an inwardly rectifying potassium channel from the basolateral membranes of *Necturus* enterocytes into planar lipid bilayers. *Proceedings of the National Academy of Sciences, USA.* 86:5212–5216.

DeCoursey, T. E., K. G. Chandy, S. Gupta, and M. D. Cahalan. Two types of potassium channels in murine T lymphocytes. *Journal of General Physiology.* 89:379–404.

Fargon, F., P. A. McNaughton, and F. V. Sepúlveda. 1990. Possible involvement of GTP-binding proteins in the deactivation of an inwardly rectifying K^+ current in enterocytes isolated from guinea-pig small intestine. *Pflügers Archiv.* 417:240–242.

Galietta, L. J. V., A. Rasola, V. Barone, D. C. Gruenert, and G. Romeo. 1991. A forskolin and verapamil sensitive K^+ current in human tracheal cells. *Biochemical and Biophysical Research Communications.* 1991:1155–1160.

Giráldez, F., and F. V. Sepúlveda. 1987. Changes in the apparent chloride permeability of *Necturus* enterocytes during the sodium-coupled transport of alanine. *Biochimica et Biophysica Acta.* 898:248–252.

Grasset, E., P. Gunter-Smith, and S. G. Schultz. 1983. Effects of Na-coupled alanine transport on intracellular K activities and the K conductance of the basolateral membranes of *Necturus* small intestine. *Journal of Membrane Biology.* 71:89–94.

Grissmer, S., and M. Cahalan. 1989. TEA prevents inactivation while blocking open K+ channels in human T lymphocytes. *Biophysical Journal.* 55:203–206.

Gunter-Smith, P. J., E. Grasset, and S. G. Schultz. 1982. Sodium-coupled amino acid and sugar transport by *Necturus* small intestine. An equivalent electrical circuit analysis of a rheogenic co-transport system. *Journal of Membrane Biology.* 66:25–39.

Hazama, A., and Y. Okada. 1988. Ca^{2+} sensitivity of volume-regulatory K+ and Cl⁻ channels in cultured human epithelial cells. *Journal of Physiology.* 402:687–702.

Hille, B. 1992. Ionic channels of excitable membranes. Second edition. Sinauer Associates Inc., Sunderland, Massachusetts.

Hodgkin, A. L., and A. F. Huxley. 1952. A quantitative description of membrane current and its application to conduction and excitation in nerve. *Journal of Physiology.* 117:500–544.

Hoshi, T., W. N. Zagotta, and R. W. Aldrich. 1990. Biophysical and molecular mechanisms of *Shaker* potassium channel inactivation. *Science.* 250:533–538.

Ilundain, A., A. I. Alcalde, Y. Barcina, and J. Larralde. 1985. Calcium-dependence of sugar transport in rat small intestine. *Biochimica et Biophysica Acta.* 818:67–72.

Kubo, M., and Y. Okada. 1992. Volume-regulatory Cl⁻ channel currents in cultured human epithelial cells. *Journal of Physiology.* 456:351–371.

Lewis, R., and M. D. Cahalan. 1988. The plasticity of ion channels: parallels between the nervous and immune systems. *Trends in Neuroscience.* 11:214–218.

MacLeod, R. J., and J. R. Hamilton. 1991a. Volume regulation initiated by Na+-nutrient cotransport in isolated mammalian villus enterocytes. *American Journal of Physiology.* 260:G26–G33.

MacLeod, R. J., and J. R. Hamilton. 1991b. Separate K+ and Cl⁻ transport pathways are activated for regulatory volume decrease in jejunal villus cells. *American Journal of Physiology.* 260:G405–G415.

Mintenig, G. M., A. S. Monaghan, and F. V. Sepúlveda. 1992. A large conductance K+-selective channel of guinea pig villus enterocytes is Ca^{2+} independent. *American Journal of Physiology.* 262:G369–G374.

Montero, M. C., M. L. Calonge, J. Bolufer, and A. Ilundain. 1990. Effect of K+ channel-blockers on sugar uptake by isolated chicken enterocytes. *Journal of Cellular Physiology.* 142:533–538.

Morris, A. P., D. V. Gallacher, and J. A. C. Lee. 1986. A large conductance, voltage- and calcium-activated K+ channel in the basolateral membrane of rat enterocytes. *FEBS Letters.* 206:87–92.

O'Brien, J. A., R. J. Walters, and F. V. Sepúlveda. 1991. Regulatory volume decrease in small intestinal crypts is inhibited by K+ and Cl⁻ channel blockers. *Biochimica et Biophysica Acta.* 1070:501–504.

Okada, Y., W. Tsuchiya, A. Irimajiri, and A. Inouye. 1977. Electrical properties and active solute transport in rat small intestine. I. Potential profile changes associated with sugar and amino acid transports. *Journal of Membrane Biology.* 31:205–219.

Rose, R. C., and S. G. Schultz. 1971. Studies on the electrical potential profile across rabbit ileum. Effects of sugars and amino acids on transmural and transmucosal electrical potential differences. *Journal of General Physiology.* 57:639–663.

Sepúlveda, F. V., F. Fargon, and P. A. McNaughton. 1991. K+ and Cl⁻ currents in enterocytes isolated from guinea-pig small intestinal villi. *Journal of Physiology.* 434:351–367.

Sheppard, D. N., F. Giráldez, and F. V. Sepúlveda. 1988a. Kinetics of voltage- and Ca^{2+} activation and Ba^{2+} blockade of a large-conductance K^+ channel from *Necturus* enterocytes. *Journal of Membrane Biology.* 105:65–75.

Sheppard, D. N., F. Giráldez, and F. V. Sepúlveda. 1988b. K^+ channels activated by L-alanine transport in isolated *Necturus* enterocytes. *FEBS Letters.* 234:446–448.

Stanfield, P. R. 1975. The effect of zinc ions on the gating of the delayed potassium conductance of frog sartorius muscle. *Journal of Physiology.* 251:711–735.

Tatsuta, H., A. Itoh, S. Ueda, and Y. Okada. 1991. Outwardly rectifying potassium currents in absorbing enterocytes isolated from the guinea pig small intestine. *Japanese Journal of Physiology.* 41:S120a. (Abstr.)

Terada, K., K. Kitamura, and H. Kuriyama. 1987. Different inhibitions of the voltage-dependent K^+ current by Ca^{2+} antagonists in the smooth muscle cell membrane of rabbit small intestine. *Pflügers Archiv.* 408:558–564.

White, J. F., and W. M. Armstrong. 1971. Effect of transported solutes on membrane potentials in bullfrog small intestine. *American Journal of Physiology.* 221:194–201.

Zagotta, W. N., T. Hoshi, and R. W. Aldrich. 1989. Gating of single *Shaker* potassium channels in *Drosophila* muscle and in *Xenopus* oocytes injected with *Shaker* mRNA. *Proceedings of the National Academy of Sciences, USA.* 86:7243–7247.

Ziomek, C. A., S. Schulman, and M. Edidin. 1980. Redistribution of membrane proteins in isolated mouse intestinal epithelial cells. *Journal of Cell Biology.* 86:849–857.